Biochemistry

Article

Cite This: Biochemistry 2019, 58, 2152−2159

pubs.acs.org/biochemistry

Structural and Functional Characterization of Sulfonium Carbon−Oxygen Hydrogen Bonding in the Deoxyamino Sugar Methyltransferase TylM1

Robert J. Fick,[†] Scott Horowitz,[‡] Brandon G. McDole,[†] Mary C. Clay,[§] Ryan A. Mehl,[∥] Hashim M. Al-Hashimi,[§] Steve Scheiner,[⊥] and Raymond C. Trievel*[,†]

[†]Department of Biological Chemistry, University of Michigan, Ann Arbor, Michigan 48109, United States

[‡]Department of Chemistry and Biochemistry, Knoebel Institute for Healthy Aging, University of Denver, Denver, Colorado 80208, United States

[§]Department of Biochemistry, Duke University, Durham, North Carolina 27710, United States

[∥]Department of Biochemistry and Biophysics, Oregon State University, Corvallis, Oregon 97331, United States

[⊥]Department of Chemistry and Biochemistry, Utah State University, Logan, Utah 84322, United States

Supporting Information

ABSTRACT: The *N*-methyltransferase TylM1 from *Streptomyces fradiae* catalyzes the final step in the biosynthesis of the deoxyamino sugar mycaminose, a substituent of the antibiotic tylosin. The high-resolution crystal structure of TylM1 bound to the methyl donor *S*-adenosylmethionine (AdoMet) illustrates a network of carbon−oxygen (CH···O) hydrogen bonds between the substrate's sulfonium cation and residues within the active site. These interactions include hydrogen bonds between the methyl and methylene groups of the AdoMet sulfonium cation and the hydroxyl groups of Tyr14 and Ser120 in the enzyme. To examine the functions of these interactions, we generated Tyr14 to phenylalanine (Y14F) and Ser120 to alanine (S120A) mutations to selectively ablate the CH···O hydrogen bonding to AdoMet. The TylM1 S120A mutant exhibited a modest decrease in its catalytic efficiency relative to that of the wild type (WT) enzyme, whereas the Y14F mutation resulted in an approximately 30-fold decrease in catalytic efficiency. In contrast, site-specific substitution of Tyr14 by the noncanonical amino acid *p*-aminophenylalanine partially restored activity comparable to that of the WT enzyme. Correlatively, quantum mechanical calculations of the activation barrier energies of WT TylM1 and the Tyr14 mutants suggest that substitutions that abrogate hydrogen bonding with the AdoMet methyl group impair methyl transfer. Together, these results offer insights into roles of CH···O hydrogen bonding in modulating the catalytic efficiency of TylM1.

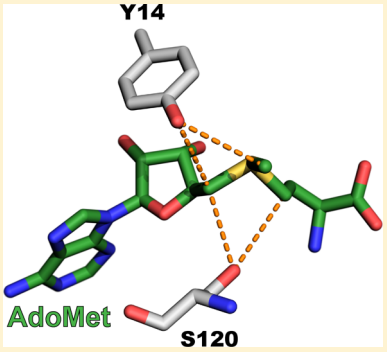

Deoxyamino sugars have garnered attention as an unusual category of carbohydrates that are synthesized in bacteria, fungi, and plants.[1] An example of a deoxyamino sugar is mycaminose, which is synthesized by *Streptomyces fradiae* as part of the biosynthetic pathway of the antibiotic Tylosin A.[2] In the final step of mycaminose synthesis, the *S*-adenosylmethionine (AdoMet)-dependent methyltransferase TylM1 methylates the amino group of dTDP-3-amino-3,6-dideoxyglucose.[3,4] The resulting product, dTDP-D-mycaminose, and two additional sugars, mycinose and mycarose, are coupled to the macrolide tylonolide to yield Tylosin A.

TylM1 is a member of the canonical Rossmann fold-like (seven-β-strand) class of methyltransferases, a large and diverse family of enzymes that methylate myriad substrates, including small molecules, metabolites, proteins, and nucleic acids.[5−7] Crystal structures of TylM1 illustrate that the enzyme comprises a catalytic domain that adopts a canonical Rossmann-like fold and a dimerization domain composed of a four-stranded antiparallel β-sheet.[8,9] AdoMet and the methyl transfer product *S*-adenosylhomocysteine (AdoHcy) bind within the catalytic domain, engaging in a network of hydrogen bonds and van der Waals interactions that are analogous to those observed in other Rossmann fold-like methyltransferases.[8] In contrast, the substrate dTDP-3-amino-3,6-dideoxyglucose is bound at the interface between the catalytic and dimerization domains, orienting its 3-amine nucleophile toward AdoMet for methyl transfer. Subsequent structural and biochemical studies have demonstrated that TylM1 can recognize and methylate a related sugar, dTDP-3-amino-3,6-dideoxygalactose, albeit with diminished activity compared to its preferred native substrate.[9]

In a survey of high-resolution crystal structures of methyltransferases belonging to different classes, TylM1 was one of more than 40 enzymes identified that displayed evidence of unconventional carbon oxygen (CH···O) hydrogen

Received: October 27, 2018
Revised: February 21, 2019
Published: February 27, 2019

DOI: 10.1021/acs.biochem.8b01141
Biochemistry 2019, 58, 2152−2159

bonding between the AdoMet sulfonium cation and residues within the active site.[10] Biochemical and biophysical characterization of these hydrogen bonds in the SET domain lysine methyltransferase (KMT) SET7/9 demonstrated that these interactions promote high-affinity binding of AdoMet.[10−12] Similarly, recent studies of the reactivation domain of cobalamin-dependent methionine synthase (MetH) have shown that water-mediated CH···O hydrogen bonding between the AdoMet sulfonium cation and glutamate residues within the enzyme's binding cleft is essential for discrimination between the substrate and the product AdoHcy.[13] Moreover, kinetic isotope effect studies of several methyltransferases have implicated CH···O interactions with the AdoMet methyl group as being important to the S_N2 reaction catalyzed by these enzymes.[14−16]

In light of these findings, we sought to expand these studies to examine the functions of these interactions in the context of a Rossmann fold-like methyltransferase. We selected TylM1 for this study because of the network of CH···O hydrogen bonding between its active site and the AdoMet sulfonium cation. Specifically, its crystal structure displays evidence of hydrogen bonding between the AdoMet methyl group and the Phe118 carbonyl group and the Tyr14 hydroxyl group. In addition, the Ser120 hydroxyl group is poised to form bifurcated CH···O hydrogen bonds with the methylene groups of the substrate's sulfonium cation. The presence of side chain-mediated hydrogen bonding affords an opportunity to characterize the functions of these interactions through site-directed mutagenesis combined with crystallographic, spectroscopic, kinetic, and computational approaches.

EXPERIMENTAL PROCEDURES

Reagents. *S*-Adenosylmethionine and *p*-aminophenylalanine were purchased from Sigma, and ThioGlo 1 was obtained from Berry & Associates. AdoMet was further purified by ion-exchange chromatography.[12,13] Isotopically labeled $^{13}CH_3$-methyl AdoMet ($^{13}CH_3$-AdoMet) was enzymatically synthesized using *Escherichia coli* AdoMet synthetase and $^{13}CH_3$-methionine (Cambridge Isotope Laboratories) and purified as previously reported.[12,13] The TylM1 substrate dTDP-3-amino-3,6-dideoxyglucose and the substrate analogue dTDP-phenol were synthesized as previously described.[8,17,18]

Protein Expression and Purification. Full length *S. fradiae* TylM1 (UniProt accession code P95748) was expressed from pET31[8] or pET24 with a C-terminal hexahistidine tag. The Y14F, Y14 to *amber*, and S120A mutants were generated using QuikChange mutagenesis (Agilent). The noncanonical amino acid *p*-aminophenylalanine (pAF) was genetically incorporated into the Y14 to *amber* mutant (TAG) utilizing *amber* stop codon suppression.[19] We previously utilized this technique to substitute an active site tyrosine by pAF in the KMT SET7/9.[11] Wild type (WT) TylM1 and the Y14F and S120A mutants were expressed in *E. coli* Rosetta 2 DE3 cells (Novagen) with overnight induction at 18 °C. The Y14pAF mutant was expressed in *E. coli* BL21-AI cells (ThermoFisher) transformed with the TylM1 Y14 to *amber* vector and the pDule2 pAF plasmid and was induced with 250 μM isopropyl β-D-1-thiogalactopyranoside, 0.2% (w/v) arabinose, and 1.0 mM pAF with overnight induction at 18 °C. WT TylM1 and its mutants were purified using TALON affinity chromatography (Clontech) followed by Superdex 200 gel filtration chromatography (GE Healthcare). The purified enzymes were concentrated and flash-frozen in liquid nitrogen before being stored at −80 °C. Protein concentrations were determined by their absorbance at 280 nm.

Nuclear Magnetic Resonance (NMR) Spectroscopy. NMR experiments were performed as described previously.[12] Samples contained 0.1 mM $^{13}CH_3$-methyl AdoMet, 0.7 mM TylM1, and 7 mM dTDP-phenol. A corresponding spectrum of TylM1 with unlabeled AdoMet was acquired as a control. Quantum mechanical (QM) optimization and NMR chemical shift calculations were performed as previously reported.[12]

Crystallization and Structure Determination. Crystals of the TylM1 Y14F, Y14pAF, and S120A mutants were obtained using the hanging drop vapor diffusion method. Crystals were grown with variable concentrations of the TylM1 mutants (18 mg/mL S120A, 12 mg/mL Y14pAF, and 9 mg/mL Y14F) in the presence of 5.0 mM AdoMet and 5.0 mM dTDP-phenol at 25 °C. Crystals of the TylM1 mutants were grown in 23−27% (w/v) PEG 3350, 100 mM HEPES (pH 7.3−7.7), 20 mM sodium malonate, 4.5−5.6 mM trimethylamine hydrochloride, and 1.0−1.25% isopropanol. Crystals were harvested in their crystallization solutions supplemented with 10% ethylene glycol and flash-frozen in liquid nitrogen. X-ray diffraction data were collected at the Advanced Photon Source Synchrotron at Sector 21, the Life Sciences Collaborative Access Team (LS-CAT). HKL2000 was used to process and scale the diffraction data.[20] Structures of the TylM1 mutants were determined by molecular replacement using Phaser with the coordinates of the TylM1/AdoMet/dTDP-phenol complex [Protein Data Bank (PDB) entry 3PFG] as the search model.[21] Model building and refinement were performed using Coot and Phenix, respectively.[22−24] During refinement, the electron density maps illustrated that the structures of the TylM1 mutants contained the product AdoHcy, potentially due to decomposition of the AdoMet. Structural figures were rendered using PyMOL (Schrödinger, LLC).

Enzyme Kinetics. The steady state kinetic parameters of WT TylM1 and its mutants were measured using a variation of an *S*-adenosylhomocysteine hydrolase (SAHH)-coupled fluorescent methyltransferase assay.[25] The assay was run in a continuous mode in which the SAHH product L-homocysteine (L-Hcy) was detected with the thiol-sensitive dye ThioGlo 1. Assays were performed in 100 mM HEPES (pH 7.5) with 5.0 μM *Solfolobus solfataricus* SAHH, 25 μM ThioGlo 1, varying concentrations of AdoMet, and 150 μM dTDP-3-amino-3,6-dideoxyglucose (apparent K_M = 23.7 μM for WT TylM1), with the exception of the Y14F mutant that was assayed with 1.5 mM dTDP-3-amino-3,6-dideoxyglucose. Assays were performed in black 384-well microplates (PerkinElmer Proxiplate 384-F) at 37 °C with enzyme concentrations from 70 to 350 nM and were initiated by the addition of AdoMet. A calibration curve of L-Hcy reacted with ThioGlo 1 was included in each microplate. The fluorescence of the adduct of ThioGlo 1 and L-Hcy was measured on a Pherastar plate reader (BMG Labtech) using a 390 nm filter for excitation and a 505 nm filter for emission. Initial velocities were measured over the first 5 min of the reactions. The Michaelis−Menten equation was fit to the kinetic data using Prism (GraphPad).

RESULTS

In the 1.3 Å resolution crystal structure of TylM1 bound to AdoMet and the substrate analogue dTDP-phenol,[8] C···O interaction distances between the AdoMet methyl group and the carbonyl group of Phe118 as well as the hydroxyl group of

DOI: 10.1021/acs.biochem.8b01141
Biochemistry 2019, 58, 2152−2159

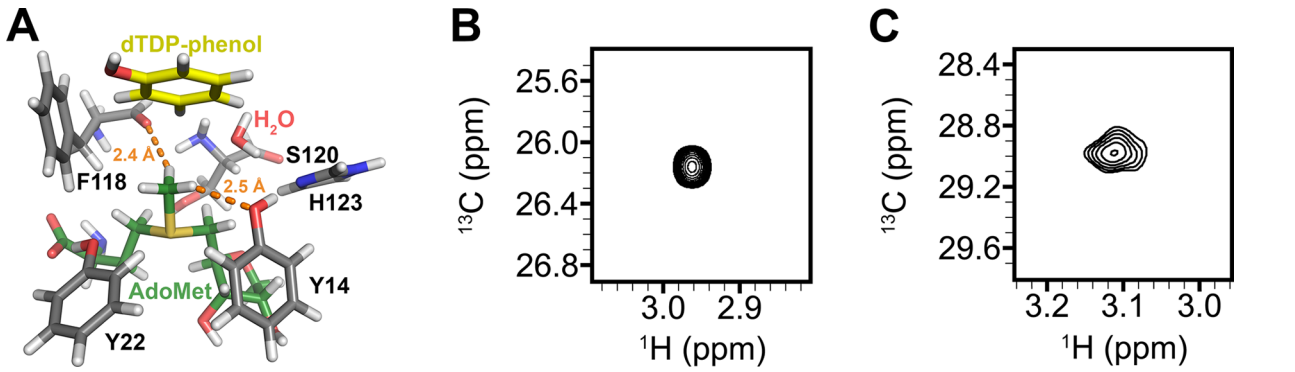

Figure 1. AdoMet methyl chemical environment probed by 2D-HSQC spectroscopy. (A) QM model of the TylM1 active site. Proposed CH···O hydrogen bonds to Phe118 and Tyr14 are depicted by orange dashes with H···O distances shown. (B) $^{13}CH_3$-AdoMet NMR spectrum in the absence of TylM1. (C) $^{13}CH_3$-AdoMet NMR spectrum in the presence of TylM1 and dTDP-phenol.

Tyr14 are consistent with CH···O hydrogen bonding (Figure 1A). However, the positions of the AdoMet methyl hydrogen atoms cannot be directly visualized at this resolution. To directly examine whether CH···O hydrogen bonding occurs between the AdoMet methyl group and the enzyme, we employed NMR spectroscopy to probe the active site environment around the methyl group. CH···O hydrogen bonding typically results in a downfield change in the ^{1}H chemical shift of the AdoMet methyl group when bound to the enzyme compared to its value free in solution.[12,26−29] We obtained a two-dimensional heteronuclear quantum coherence (2D-HSQC) spectrum of $^{13}CH_3$-AdoMet bound to TylM1 to measure the ^{1}H chemical shift of its methyl group. The 2D-HSQC spectrum showed a downfield change in the ^{1}H chemical shift of $^{13}CH_3$-AdoMet (Figure 1B,C and Table 1)

Table 1. Calculated and Experimental ^{1}H Chemical Shifts of $^{13}CH_3$-AdoMet in Solution and Bound to TylM1

AdoMet environment	calculated chemical shift (ppm)	experimental chemical shift (ppm)
TylM1 active site	3.4	3.1
class I pose	2.7	not determined
aqueous	3.0[a]	3.0

[a]Reproduced from ref 12.

when bound to the enzyme. However, this change was smaller than that observed for $^{13}CH_3$-AdoMet bound to SET7/9, which exhibits relatively strong CH···O hydrogen bonding to the substrate.[12] Density functional theory (DFT) calculations on AdoMet in isolation demonstrated that the smaller chemical shift change arose from the conformation that AdoMet adopts when bound in the active site of TylM1. The pose assumed by AdoMet shifts the methyl hydrogen resonances substantially upfield from the pose assumed by AdoMet when free in aqueous solution (Table 1).[12,30] The total change in the ^{1}H chemical shift of the AdoMet methyl hydrogens therefore appears to be small, as the upfield chemical shift change caused by the change in conformation partially cancels out the downfield chemical shift change caused by the CH···O hydrogen bonding. Nonetheless, the observed downfield ^{1}H chemical shift change with the DFT calculations strongly implies the formation of CH···O hydrogen bonding between the AdoMet methyl group and the active site of TylM1.

After examining CH···O hydrogen bonding by NMR spectroscopy, we investigated the functions of the hydrogen bond acceptors Tyr14 and Ser120 in TylM1 through site-directed mutagenesis and steady state kinetic analysis. A Ser120 to alanine (S120A) mutation was generated to ablate CH···O hydrogen bonding to the methylene groups of the AdoMet sulfonium cation, whereas a Tyr14 to phenylalanine substitution (Y14F) abolished hydrogen bonding to the methyl and a methylene group in the substrate (Figure 2A and Figure S1A). In addition, we site-specifically substituted Tyr14 with *p*-amino-L-phenylalanine (Y14pAF), the aniline analogue of tyrosine, using an *amber* codon suppression strategy commonly employed to genetically incorporate noncanonical amino acids into proteins.[19] This substitution would potentially maintain the hydrogen bond with the imidazole group of His123 that is disrupted by the Y14F mutation. In prior studies, we utilized an analogous tyrosine to pAF substitution to probe the functions of CH···O hydrogen bonding to AdoMet in SET7/9.[11] To ascertain whether these substitutions alter the overall conformation of the enzyme or its active site, we determined crystal structures of the TylM1 Y14F, Y14pAF, and S120A mutants bound to dTDP-phenol and AdoHcy (Table S1). An alignment of the structures of Tyr14 and Ser120 mutants to WT TylM1 illustrates their overall structural homology [root-mean-square deviation (RMSD) for aligned Cα atoms of <0.5 Å] and that the mutants preserve the active site structure of the WT enzyme (Figure 2B−D and Figure S1B−D). Notably, the NH···O hydrogen bond between the side chains of Tyr14 and His123 in WT TylM1 is preserved as an NH···N hydrogen bond in the Y14pAF mutant (Figure 2D and Figure S1D), as anticipated for this substitution.

Following structure determination, we determined the kinetic parameters of WT TylM1 and the Tyr14 and Ser120 mutants for AdoMet (Figure 3). The k_{cat} and K_M values measured for the WT enzyme (Table 2) are similar to those previously reported.[8] The catalytic efficiency (k_{cat}/K_M) of the TylM1 S120A mutant was diminished by approximately 4-fold compared to that of the WT enzyme, because of a 2-fold decrease in k_{cat} and a 2-fold increase in the K_M value for AdoMet. Similarly, the TylM1 Y14pAF mutant also displayed an approximately 4-fold decrease in catalytic efficiency. However, this reduction was primarily a consequence of a diminished turnover number, as there was a negligible effect on the K_M value of AdoMet compared to that of the WT enzyme. This finding indicates that the amine moiety of pAF was able to at least partially substitute for the Tyr14 hydroxyl group,

DOI: 10.1021/acs.biochem.8b01141
Biochemistry 2019, 58, 2152−2159

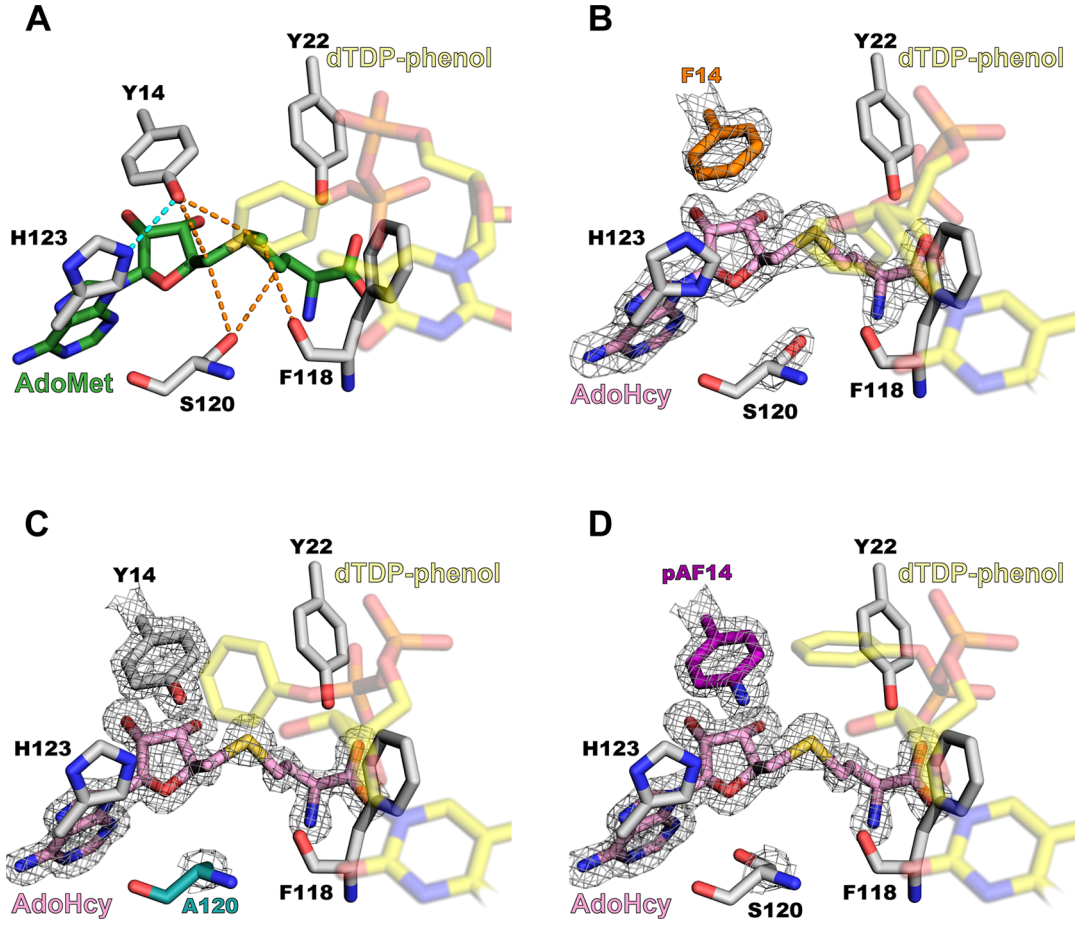

Figure 2. Crystal structures of WT TylM1 and the Tyr14 and Ser120 mutants. (A) Active site of the previously reported structure of the WT TylM1/AdoMet/dTDP-phenol ternary complex (PDB entry 3PFG). The carbon atoms of AdoMet and dTDP-phenol are colored green and yellow, respectively. The dTDP-phenol is rendered semitransparently to allow visualization of AdoMet and the surrounding active site residues. CH···O and conventional hydrogen bonds are depicted as orange and cyan dashes, respectively. (B) Crystal structure of the TylM1 Y14F/AdoHcy/dTDP-phenol complex. The Y14F substitution is denoted by orange carbon atoms, and AdoHcy is shown with pink carbon atoms. The $F_o - F_c$ simulated annealing omit map is rendered around Phe14, AdoHcy, and Ser120 and is contoured at 3.0σ. (C) Structure of the TylM1 S120A/AdoHcy/dTDP-phenol complex. The S120A mutation is highlighted with cyan carbon atoms. (D) Structure of the TylM1 pAF14/AdoHcy/dTDP phenol complex. The Y14pAF mutation is depicted with purple carbon atoms.

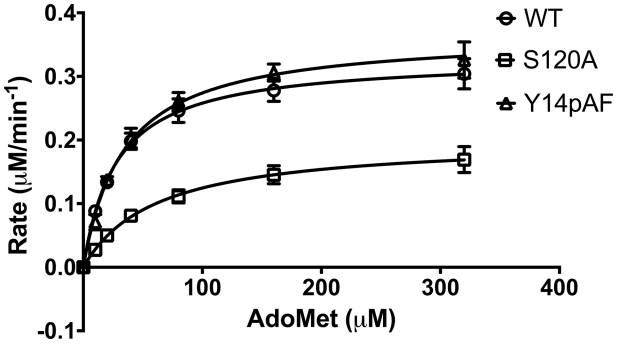

Figure 3. Steady state kinetic analysis of WT TylM1 (○), the TylM1 S120A mutant (□), and the TylM1 Y14pAF mutant (△).

Table 2. Kinetic Analysis of WT TylM1 and the Tyr14 and Ser120 Mutants at 37 °C

TylM1	k_{cat} (min^{-1})	K_M, AdoMet (μM)	k_{cat}/K_M (M^{-1} min^{-1})
WT	4.71 ± 0.04	27.8 ± 0.9	169000 ± 6000
Y14F	1.21 ± 0.03	212 ± 12	5730 ± 350
Y14pAF	1.75 ± 0.04	34.0 ± 2.4	51400 ± 3800
S120A	2.87 ± 0.03	61.5 ± 1.8	46700 ± 1500

consistent with the structure of this mutant (Figure 2D and Figure S1D). In contrast, the TylM1 Y14F mutant exhibited an ~30-fold decrease in catalytic efficiency relative to that of the WT enzyme (Figure S2). This decrease was due to a 4-fold decrease in k_{cat} and a 7.5-fold increase in the K_M value for AdoMet. Thus, the loss of hydrogen bonding associated with the Y14F mutant was deleterious for activity in TylM1, whereas the Y14pAF mutation partially restored activity.

We next examined whether disruption of the CH···O hydrogen bonding between the Tyr14 and the AdoMet methyl group would affect methyl transfer using computational chemistry. To facilitate the QM calculations, minimal active site models for WT TylM1 and the Y14F and Y14pAF mutants bound to the substrates were generated (Figure 4 and Figure S3; see the Supplemental Methods in the Supporting Information for a description of the QM calculations and generation of the active site models). In these active site models, the motion of the methyl group from the AdoMet model to the nitrogen atom on 3-amino-3,6-dideoxyglucose traced out a methyl transfer potential (Figure 5 and Figure S4).

DOI: 10.1021/acs.biochem.8b01141
Biochemistry 2019, 58, 2152−2159

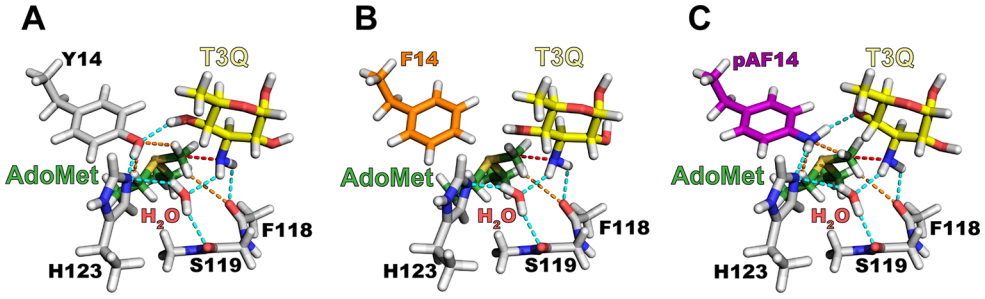

Figure 4. Active site models of the TylM1 substrate complexes used in the QM calculations of the methyl transfer reaction for (A) WT TylM1, (B) the TylM1 Y14F mutant, and (C) the TylM1 Y14pAF mutant. AdoMet and 3-amino-3,6-dideoxyglucose (T3Q) are denoted by green and yellow carbon atoms, respectively. CH···O and conventional hydrogen bonds are depicted by orange and cyan dashed lines, respectively. The reaction coordinate for methyl transfer is shown by red dashed lines.

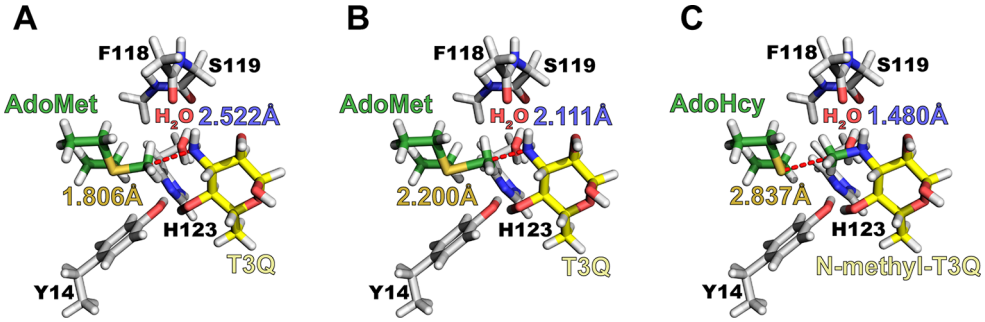

Figure 5. Snapshots from the QM calculations of methyl transfer for WT TylM1: (A) AdoMet/T3Q substrate complex, (B) transition state, and (C) AdoHcy/3-*N*-methylamino-3,6-dideoxyglucose (*N*-methyl-T3Q) product complex. The dashed red line illustrates either the methyl carbon–nitrogen or methyl carbon–sulfur interaction proceeding from the substrate complex through the transition state to the product complex with the C–S and C–N distances denoted in yellow and blue text, respectively.

The height of the activation barrier for methyl transfer from the sulfur atom of $MeS^{+}(Et)_2$ to the nitrogen atom of the sugar substrate is denoted by $E^{\dagger}$ in Table 3, and the overall energy of this transfer is represented as ΔE. As one can see from the last column of Table 3, this transfer is exothermic in all cases by approximately −20 kcal/mol, suggesting the methyl group prefers association with the nitrogen atom over the sulfur atom by this amount of energy. The exothermicity associated with the models of the WT enzyme and the Y14F mutant is relatively similar but is reduced for the Y14pAF mutant. An analysis of the WT enzyme indicates that the CH···O hydrogen bond between the Tyr14 hydroxyl group and the transferring methyl group is preserved between the substrate and product complexes and therefore does not substantially affect the overall methyl transfer energy. The Y14F mutant lacks this interaction, and thus, it does not contribute to the ΔE for this mutant. In contrast, the exothermicity of the Y14pAF mutant is decreased due to the formation of a CH···N hydrogen bond between the transferring methyl group and the pAF aniline side chain, which is strongest with the AdoMet methyl group and weaker in the product complex, diminishing the value of ΔE. The energy barrier impeding this S → N methyl transfer occurs when the R(S–C) distance has elongated by 0.4 Å from 1.8 to 2.2 Å. The energy barrier is 8.1 kcal/mol for WT TylM1 but increases to >9 kcal/mol for the two Tyr14 mutants. There is a general correlation that may be noted between these two quantities in that a more negative ΔE value is associated with a lower barrier (Table 3). The activation barriers for the Y14F and Y14pAF mutants, which are roughly comparable to one another, are larger than the barrier for the WT enzyme, consistent with the diminished k_{cat} values for the mutants (Table 2).

Table 3. QM Calculations of the Activation Barriers ($E^{\dagger}$) and Overall Methyl Transfer Energies (ΔE) for WT TylM1 and the Tyr14 Mutants

TylM1	$E^{\dagger}$ (kcal/mol)	ΔE (kcal/mol)
WT	8.1	−24.7
Y14F	9.6	−24.1
Y14pAF	9.3	−21.5

Insight into the effect of the mutations on the reaction rate can be gleaned through examination of the CH···O hydrogen bonds involving the transferring methyl group. In the ground and transition state configurations of the WT model, there are several CH···O hydrogen bonds in evidence that involve the methyl protons (Figures 4A and 5 and Figures S3A and S4). One of the methyl hydrogen atoms lies within 2.5 Å of the carbonyl oxygen of Phe118, while a second methyl proton is within 2.3 Å of the hydroxyl group of Tyr14. It is the latter interaction that is disrupted in the Tyr14 mutants. The Y14F mutation abolishes the CH···O hydrogen bond to the AdoMet methyl group and also disrupts hydrogen bonding to the imidazole of His123 and the C4′ hydroxyl group of the 3-amino-3,6-dideoxyglucose substrate (Figure 4B and Figure S3B). The substitution of Tyr14 with pAF has a more nuanced effect on interactions within the active site. The amino group of the pAF side chain preserves hydrogen bonding to His123 and the C4′ hydroxyl group of the sugar substrate and also accepts an OH···N hydrogen bond from the active site water molecule (Figure 4C and Figure S3C). These interactions,

DOI: 10.1021/acs.biochem.8b01141
Biochemistry 2019, 58, 2152–2159

coupled with the sp^2 hybridization of the pAF amino nitrogen atom that delocalizes its lone pair of electrons into the phenyl ring, weaken any potential CH···N hydrogen bonding between pAF14 and the methyl group of AdoMet. In summary, these observations provide an explanation of how disruption of methyl CH···O hydrogen bonding in the TylM1 Tyr14 mutants increases the activation barrier $E^{\dagger}$ for methyl transfer and lowers the exothermicity of the reaction.

DISCUSSION

The structural and functional characterization of Tyr14 and Ser120 in TylM1 provides a framework for understanding the functions of these residues in CH···O hydrogen bonding with the AdoMet sulfonium cation. The TylM1 S120A mutant displayed modest defects in the K_M value for AdoMet and k_{cat} (Table 2), indicating that the Ser120 hydroxyl group may have a subtle role in substrate recognition and turnover in the enzyme. Substitutions of Tyr14 by phenylalanine and pAF resulted in similar decreases in k_{cat}, whereas the Y14F mutant also diminished the K_M value for AdoMet compared to those of the WT enzyme and the Y14pAF mutant. It is also worth noting that Tyr14 participates in an OH···O hydrogen bond with the C4′-hydroxyl group in dTDP-3-amino-3,6-dideoxyglucose and an OH···N hydrogen bond with the imidazole of His123 (Figure 4A and Figure S3A). Biochemical characterization of an alternative substrate, dTDP-3-amino-3,4,6-trideoxyglucose, which lacks the C4′-hydroxyl group, demonstrated that it was methylated by TylM1 with a catalytic efficiency approximately 2-fold lower than that of the native substrate,[31] implying that the OH···O hydrogen bond with Tyr14 is not essential for substrate binding and catalysis. On the other hand, previous kinetic studies have demonstrated that mutations of His123 in TylM1 diminished the catalytic efficiency by 1−2 orders of magnitude.[8] These findings led to the proposal that the His123 imidazole group may function in water-mediated deprotonation of the C3′-amino group of the sugar prior to methyl transfer. Thus, the hydrogen bond between Tyr14 and His123 may play a role in facilitating water-mediated deprotonation of the substrate, potentially by orienting its imidazole group for shuttling protons from the substrate to bulk solvent.

The results of these studies also offer an opportunity to compare and contrast the properties and functions of CH···O hydrogen bonding among different methyltransferases. In the 2D-HSQC spectroscopy experiments, a range of ^{1}H chemical shifts for the AdoMet methyl group have been reported for different methyltransferases.[10,12,13] In the model SET domain KMT SET7/9, the AdoMet methyl group exhibited a ^{1}H chemical shift of 3.7 ppm when bound in the enzyme's active site.[12] This shift is markedly downfield of the methyl ^{1}H chemical shift for AdoMet free in solution [3.0 ppm (Table 1)] and is indicative of either strong or extensive methyl CH···O hydrogen bonding between the AdoMet methyl group and SET7/9. In agreement with this observation, DFT calculations suggested three CH···O hydrogen bonds (Figure S5A) to the AdoMet methyl group formed by the carbonyl groups of Gly264 and His293 and the hydroxyl group of the invariant Tyr335 in SET7/9, with hydrogen bond (H···O) distances of 2.7, 2.1, and 2.5 Å, respectively.[12] Consistent with these results, mutation of Tyr335 to phenylalanine in SET7/9, which abolishes one of the CH···O hydrogen bonds to the AdoMet methyl group, resulted in a slightly smaller downfield change in the methyl ^{1}H chemical shift to 3.6 ppm.[10] This relatively small alteration in the chemical shift compared to that of the WT enzyme suggests that the interaction between the Tyr335 hydroxyl group and the AdoMet methyl group is weaker than the CH···O hydrogen bonds with carbonyl groups of Gly264 and His293, particularly with the latter given its short hydrogen bond distance (2.1 Å).

In contrast to that of SET7/9, the ^{1}H chemical shift measured for $^{13}CH_3$-AdoMet bound to TylM1 is 3.1 ppm (Table 1). This modest change in the chemical shift is in part due to the change in the conformation of AdoMet from its free state in solution to its enzyme-bound state. In addition, the smaller change in the chemical shift may be a consequence of fewer and generally longer CH···O hydrogen bonds between the AdoMet methyl group and the active site residues in TylM1 (Figure 1A and Figure S5B) compared to SET7/9 (Figure S5A). On the other hand, 2D-HSQC spectroscopy experiments with the reactivation domain of methionine synthase (MetH) demonstrated that the methyl ^{1}H chemical shift of AdoMet was essentially unaltered upon association with the enzyme (3.0 ppm).[13] This finding is consistent with the solvent-exposed substrate binding site of MetH, in which the only interactions with the AdoMet methyl group involve water-mediated CH···O hydrogen bonds with active site residues. Together, these results illustrate that the ^{1}H chemical shift of the AdoMet methyl group reflects the CH···O hydrogen bonding environment within the methyltransferase active site and thus can be employed as a sensitive probe that reports on the number and relative strength of these interactions.

A comparison of the effects of active site tyrosine mutations in SET7/9 and TylM1 furnishes insights into the roles of methyl CH···O hydrogen bonding in the kinetics of methyl transfer. In SET7/9, the invariant Tyr335 engages in a network of CH···O hydrogen bonds with AdoMet, including the methyl and methylene groups of the sulfonium cation, as well as the C8 atom of the adenine ring (Figure S5A).[10] Mutations of Tyr335 to phenylalanine and pAF increased the K_M value for AdoMet by ∼60- and ∼130-fold, respectively, compared to that of WT SET7/9.[10,11] Conversely, the Y14F mutation in TylM1 resulted in a modest increase in the K_M value for AdoMet, whereas the Y14pAF mutation essentially had no effect on the K_M (Table 2). These differences are a manifestation of the different CH···O hydrogen bonding patterns present in the respective active sites of the two enzymes (Figure S5). In SET7/9, Tyr335 participates in multiple CH···O hydrogen bonds with the sulfonium and adenine moieties of AdoMet, and mutations of this residue resulted in substantial increases in the K_D and K_M values of the substrate.[10] Conversely, Tyr14 forms hydrogen bonds with the methyl group and a methylene group in AdoMet, and substitutions of this residue lead to more modest changes in K_M.

With respect to turnover, the SET7/9 Y335pAF mutation diminished k_{cat} by 35-fold compared to that of WT SET7/9, whereas the Y335F mutation had a <2-fold effect on k_{cat}. In TylM1, the Y14F and Y14pAF mutations resulted in modest reductions in the k_{cat} value (Table 2). Collectively, these tyrosine mutations indicate that their methyl CH···O hydrogen bonds with AdoMet may influence the methyl transfer rate, consistent with the QM calculations of the methyl transfer reaction energies for WT TylM1 and the Tyr14 mutants (Table 3). However, it is conceivable that deprotonation of the nucleophilic amino group in dTDP-3-amino-3,6-dideoxyglu-

DOI: 10.1021/acs.biochem.8b01141
Biochemistry 2019, 58, 2152−2159

cose is rate-limiting in TylM1. Thus, the effects of the Tyr14 mutants could be underestimated in the kinetic experiments if these mutations slow methyl transfer to the point of being at least partially rate-limiting. It may also be worth mentioning that the quantum calculations of the methyl transfer potentials were performed with certain limitations, such as restricting the methyl C to the S−N axis, and holding certain other atoms fixed during the process.

It is worth noting that carbonyl groups of active site residues in SET7/9 and TylM1 (Figure S5) also participate in AdoMet methyl CH···O hydrogen bonding.[10,12] Prior QM calculations have demonstrated that the carbonyl oxygen atom in a model peptide forms CH···O hydrogen bonds with a sulfonium model of AdoMet that are approximately 3-fold stronger than the interactions with the hydroxyl group of phenol, representing the side chain of tyrosine.[10] The functions of these carbonyl groups engaging in methyl CH···O hydrogen bonding have not been experimentally investigated to date, in part because they cannot be directly characterized by conventional biochemical approaches utilizing site-directed mutagenesis. It is conceivable that the interactions between these carbonyl groups and AdoMet may play a compensatory role in active site mutations that ablate methyl CH···O hydrogen bonding, such as those involving tyrosine or other polar amino acids. For example, the Y335F mutation in SET7/9 resulted in a <2-fold effect on k_{cat} and an only 0.1 ppm upfield change for the methyl ^{1}H chemical shift of AdoMet compared to those of the WT enzyme.[10] The aforementioned CH···O hydrogen bond between the AdoMet methyl group and the His293 carbonyl oxygen atom is shorter and presumably stronger than the hydrogen bond with Tyr335, implying that the interaction with His293 may be more important to the observed downfield change in the methyl ^{1}H chemical shift and transition state stabilization in SET7/9 (Figure S5A).[10,12] Similarly, recent computational studies investigating the reaction mechanism of glycine *N*-methyltransferase have shown that mutations of Tyr21 that abolish AdoMet methyl CH···O interactions in the transition state are compensated by the methyl group's interactions with the imidazole of His142 and the carbonyl oxygen of Gly137.[16] Future studies focusing on the characterization of CH···O hydrogen bonding between AdoMet and active site carbonyl groups will be essential in elucidating the contributions of these interactions to substrate recognition and catalysis.

■ ASSOCIATED CONTENT

Supporting Information

The Supporting Information is available free of charge on the ACS Publications website at DOI: 10.1021/acs.biochem.8b01141.

Methods for computational chemistry; table reporting the crystallographic and refinement statistics; and figures illustrating the kinetic analysis of the TylM1 Y14F mutant, stereo representations of the TylM1 active site and models for the QM calculations, and a comparison of CH···O hydrogen bonding between the active sites of TylM1 and SET7/9 (PDF)

Accession Codes

Coordinates and structure factors for the TylM1 Y14F/SAH/dTDP-phenol (6M81), TylM1 Y14pAF/SAH/dTDP-phenol (6M82), and TylM1 S120A/SAH/dTDP-phenol (6M83) ternary complexes have been deposited in the RCSB PDB.

■ AUTHOR INFORMATION

Corresponding Author

*Department of Biological Chemistry, University of Michigan, 1150 W. Medical Center Dr., 5301 Medical Science Research Building 3, Ann Arbor, MI 48109. E-mail: rtrievel@umich.edu. Phone: 734-647-0889. Fax: 734-763-4581.

ORCID

Ryan A. Mehl: 0000-0003-2932-4941
Steve Scheiner: 0000-0003-0793-0369
Raymond C. Trievel: 0000-0003-3189-8792

Funding

These studies were supported by National Science Foundation Grant CHE-1508492 to H.M.A.-H. and R.C.T.

Notes

The authors declare no competing financial interest.

■ ACKNOWLEDGMENTS

The authors thank H. Holden and J. Thoden (University of Wisconsin) for providing the expression vector for TylM1 and for their generous gift of dTDP-phenol and dTDP-3-amino-3,6-dideoxyglucose. This research used resources of the Advanced Photon Source, a U.S. Department of Energy (DOE) Office of Science User Facility operated for the DOE Office of Science by Argonne National Laboratory under Contract DE-AC02-06CH11357. Use of LS-CAT Sector 21 was supported by the Michigan Economic Development Corp. and the Michigan Technology Tri-Corridor (Grant 085P1000817).

■ REFERENCES

(1) Nedal, A., and Zotchev, S. B. (2004) Biosynthesis of deoxyaminosugars in antibiotic-producing bacteria. *Appl. Microbiol. Biotechnol. 64*, 7−15.

(2) Arsic, B., Barber, J., Cikos, A., Mladenovic, M., Stankovic, N., and Novak, P. (2018) 16-membered macrolide antibiotics: a review. *Int. J. Antimicrob. Agents 51*, 283−298.

(3) Gandecha, A. R., Large, S. L., and Cundliffe, E. (1997) Analysis of four tylosin biosynthetic genes from the tylLM region of the Streptomyces fradiae genome. *Gene 184*, 197−203.

(4) Melancon, C. E., 3rd, Yu, W. L., and Liu, H. W. (2005) TDP-mycaminose biosynthetic pathway revised and conversion of desosamine pathway to mycaminose pathway with one gene. *J. Am. Chem. Soc. 127*, 12240−12241.

(5) Schubert, H. L., Blumenthal, R. M., and Cheng, X. (2003) Many paths to methyltransfer: a chronicle of convergence. *Trends Biochem. Sci. 28*, 329−335.

(6) Petrossian, T., and Clarke, S. (2009) Bioinformatic Identification of Novel Methyltransferases. *Epigenomics 1*, 163−175.

(7) Petrossian, T. C., and Clarke, S. G. (2011) Uncovering the Human Methyltransferasome. *Mol. Cell. Proteomics 10*, M110.000976.

(8) Carney, A. E., and Holden, H. M. (2011) Molecular architecture of TylM1 from Streptomyces fradiae: an N,N-dimethyltransferase involved in the production of dTDP-D-mycaminose. *Biochemistry 50*, 780−787.

(9) Thoden, J. B., and Holden, H. M. (2014) Production of a novel N-monomethylated dideoxysugar. *Biochemistry 53*, 1105−1107.

(10) Horowitz, S., Dirk, L. M., Yesselman, J. D., Nimtz, J. S., Adhikari, U., Mehl, R. A., Scheiner, S., Houtz, R. L., Al-Hashimi, H. M., and Trievel, R. C. (2013) Conservation and functional importance of carbon-oxygen hydrogen bonding in AdoMet-dependent methyltransferases. *J. Am. Chem. Soc. 135*, 15536−15548.

(11) Horowitz, S., Adhikari, U., Dirk, L. M., Del Rizzo, P. A., Mehl, R. A., Houtz, R. L., Al-Hashimi, H. M., Scheiner, S., and Trievel, R. C. (2014) Manipulating unconventional CH-based hydrogen bonding in

DOI: 10.1021/acs.biochem.8b01141
Biochemistry 2019, 58, 2152−2159

a methyltransferase via noncanonical amino acid mutagenesis. *ACS Chem. Biol. 9*, 1692−1697.
(12) Horowitz, S., Yesselman, J. D., Al-Hashimi, H. M., and Trievel, R. C. (2011) Direct evidence for methyl group coordination by carbon-oxygen hydrogen bonds in the lysine methyltransferase SET7/9. *J. Biol. Chem. 286*, 18658−18663.
(13) Fick, R. J., Clay, M. C., Vander Lee, L., Scheiner, S., Al-Hashimi, H., and Trievel, R. C. (2018) Water-Mediated Carbon-Oxygen Hydrogen Bonding Facilitates S-Adenosylmethionine Recognition in the Reactivation Domain of Cobalamin-Dependent Methionine Synthase. *Biochemistry 57*, 3733−3740.
(14) Poulin, M. B., Schneck, J. L., Matico, R. E., McDevitt, P. J., Huddleston, M. J., Hou, W., Johnson, N. W., Thrall, S. H., Meek, T. D., and Schramm, V. L. (2016) Transition state for the NSD2-catalyzed methylation of histone H3 lysine 36. *Proc. Natl. Acad. Sci. U. S. A. 113*, 1197−1201.
(15) Linscott, J. A., Kapilashrami, K., Wang, Z., Senevirathne, C., Bothwell, I. R., Blum, G., and Luo, M. (2016) Kinetic isotope effects reveal early transition state of protein lysine methyltransferase SET8. *Proc. Natl. Acad. Sci. U. S. A. 113*, E8369−E8378.
(16) Swiderek, K., Tunon, I., Williams, I. H., and Moliner, V. (2018) Insights on the Origin of Catalysis on Glycine N-Methyltransferase from Computational Modeling. *J. Am. Chem. Soc. 140*, 4327−4334.
(17) Zhao, Y., and Thorson, J. S. (1998) A Methodological Comparison: The Advantage of Phosphorimidates in Expanding the Sugar Nucleotide Repertoire. *J. Org. Chem. 63*, 7568−7572.
(18) Giraud, M. F., Leonard, G. A., Field, R. A., Berlind, C., and Naismith, J. H. (2000) RmlC, the third enzyme of dTDP-L-rhamnose pathway, is a new class of epimerase. *Nat. Struct. Biol. 7*, 398−402.
(19) Mehl, R. A., Anderson, J. C., Santoro, S. W., Wang, L., Martin, A. B., King, D. S., Horn, D. M., and Schultz, P. G. (2003) Generation of a bacterium with a 21 amino acid genetic code. *J. Am. Chem. Soc. 125*, 935−939.
(20) Otwinowski, Z., and Minor, W. (1997) Processing of X-ray diffraction data collected in oscillation mode. *Methods Enzymol. 276*, 307−326.
(21) Mccoy, A. J., Grosse-Kunstleve, R. W., Adams, P. D., Winn, M. D., Storoni, L. C., and Read, R. J. (2007) Phaser crystallographic software. *J. Appl. Crystallogr. 40*, 658−674.
(22) Emsley, P., and Cowtan, K. (2004) Coot: model-building tools for molecular graphics. *Acta Crystallogr., Sect. D: Biol. Crystallogr. 60*, 2126−2132.
(23) Emsley, P., Lohkamp, B., Scott, W. G., and Cowtan, K. (2010) Features and development of Coot. *Acta Crystallogr., Sect. D: Biol. Crystallogr. 66*, 486−501.
(24) Adams, P. D., Afonine, P. V., Bunkoczi, G., Chen, V. B., Davis, I. W., Echols, N., Headd, J. J., Hung, L. W., Kapral, G. J., Grosse-Kunstleve, R. W., McCoy, A. J., Moriarty, N. W., Oeffner, R., Read, R. J., Richardson, D. C., Richardson, J. S., Terwilliger, T. C., and Zwart, P. H. (2010) PHENIX: a comprehensive Python-based system for macromolecular structure solution. *Acta Crystallogr., Sect. D: Biol. Crystallogr. 66*, 213−221.
(25) Collazo, E., Couture, J. F., Bulfer, S., and Trievel, R. C. (2005) A coupled fluorescent assay for histone methyltransferases. *Anal. Biochem. 342*, 86−92.
(26) Ash, E. L., Sudmeier, J. L., Day, R. M., Vincent, M., Torchilin, E. V., Haddad, K. C., Bradshaw, E. M., Sanford, D. G., and Bachovchin, W. W. (2000) Unusual H-1 NMR chemical shifts support (His) C-epsilon 1-H center dot center dot center dot O = C H-bond: Proposal for reaction-driven ring flip mechanism in serine protease catalysis. *Proc. Natl. Acad. Sci. U. S. A. 97*, 10371−10376.
(27) Peralta, J. E., Ruiz de Azua, M. C., and Contreras, R. H. (1999) Natural bond orbitals analysis of C-H center dot center dot center dot O interactions in NCH/H2O and NCH/OCH2, and their effect on nuclear magnetic shielding constants. *J. Mol. Struct.: THEOCHEM 491*, 23−31.
(28) Scheiner, S., Gu, Y., and Kar, T. (2000) Evaluation of the H-bonding properties of CH center dot center dot center dot O interactions based upon NMR spectra. *J. Mol. Struct.: THEOCHEM 500*, 441−452.
(29) Afonin, A. V., Ushakov, I. A., Kuznetsova, S. Y., Petrova, O. V., Schmidt, E. Y., and Mikhaleva, A. I. (2002) C-H center dot center dot center dot X (X = N, O, S) intramolecular interaction in 1-vinyl-2-(2'-heteroaryl)pyrroles as monitored by H-1 and C-13 NMR spectroscopy. *Magn. Reson. Chem. 40*, 114−122.
(30) Markham, G. D., Norrby, P. O., and Bock, C. W. (2002) S-adenosylmethionine conformations in solution and in protein complexes: conformational influences of the sulfonium group. *Biochemistry 41*, 7636−7646.
(31) Chen, H., Yamase, H., Murakami, K., Chang, C. W., Zhao, L., Zhao, Z., and Liu, H. W. (2002) Expression, purification, and characterization of two N,N-dimethyltransferases, tylM1 and desVI, involved in the biosynthesis of mycaminose and desosamine. *Biochemistry 41*, 9165−9183.

DOI: 10.1021/acs.biochem.8b01141
Biochemistry 2019, 58, 2152−2159